Author Manuscript

Author Manuscript

Author Manuscript

Author Manuscript

HHS Public Access

Author manuscript

J Endocrinol. Author manuscript; available in PMC 2016 March 22.

Published in final edited form as:

J Endocrinol. 2016 January ; 228(1): 49–59. doi:10.1530/JOE-15-0288.

Prediabetes Linked to Excess Glucagon in Transgenic Mice with Pancreatic Active AKT1

Toya M. Albury-Warren[1], **Veethika Pandey**[1], **Lina P. Spinel**[1], **Michal M. Masternak**[1,2], and **Deborah A Altomare**[1]

[1]University of Central Florida, College of Medicine, Burnett School of Biomedical Sciences, 6900 Lake Nona Blvd. Orlando, FL 32827, USA [2]Department of Head and Neck Surgery, The Greater Poland Cancer Centre, 61-866 Poznan, Poland

Abstract

Protein Kinase B/AKT, has three isoforms (AKT1-3) and is renowned for its central role in the regulation of cell growth and proliferation, due to its constitutive activation in various cancers. AKT2, which is highly expressed in insulin responsive tissues, has been identified as a primary regulator of glucose metabolism as *Akt2* knockout mice (*Akt2*$^{-/-}$) are glucose intolerant and insulin resistant. However, the role of AKT1 in glucose metabolism is not as clearly defined. We previously showed that mice with myristoylated *Akt1* (AKT1^{Myr}) expressed through a bicistronic *Pdx1-TetA* and *TetO-MyrAkt1* system were susceptible to islet cell carcinomas, and in this study we characterized an early onset, prediabetic phenotype. Beginning at weaning (3 weeks of age), the glucose intolerant AKT1^{Myr} mice exhibited non-fasted hyperglycemia, which progressed to fasted hyperglycemia by 5 months of age. The glucose intolerance was attributed to a fasted hyperglucagonemia, and hepatic insulin resistance detectable by reduced phosphorylation of the insulin receptor following insulin injection into the inferior vena cava. In contrast, treatment with doxycycline diet to turn-off the transgene, caused attenuation of the non-fasted and fasted hyperglycemia, thus affirming AKT1 hyperactivation as the trigger. Collectively, this model highlights a novel glucagon-mediated mechanism by which AKT1 hyperactivation affects glucose homeostasis, and provides an avenue to better delineate the molecular mechanisms responsible for diabetes mellitus and the potential association with pancreatic cancer.

Keywords

Insulin signaling; glucagon; glucose metabolism; pancreas; oncogenes

Corresponding Author: Dr. Deborah A Altomare, Ph.D., University of Central Florida, College of Medicine, Burnett School of Biomedical Sciences, 6900 Lake Nona Blvd. Orlando, FL 32827, USA, Deborah.Altomare@ucf.edu.

Declaration of Interests

There are no conflicts of interest biasing the research reported.

Author Contribution Statement

T.M.A, the first author, designed the study, performed all of the experiments, and prepared this manuscript. V.P assisted in all of the metabolism studies (GTT, ITT, and insulin stimulation). L.S. assisted with breeding, weaning, genotyping, and glucose testing. M.M.M served as an expert consultant on all metabolism experiments. D.A.A., the corresponding author, provided financial support and supervised the project. All authors were involved in the editing of this manuscript.

Author Manuscript Author Manuscript Author Manuscript Author Manuscript

Introduction

AKT, a serine/threonine kinase, is downstream of phosphatidylinositol 3-kinase (PI3K) and growth factor receptors (e.g., epidermal growth factor receptor, EGFR), and is a hallmark signaling protein predominantly recognized for regulation of cell survival, growth, and proliferation. AKT signals through the phosphorylation and subsequent activation or inhibition of downstream substrates, such as mammalian target of rapamycin complex 1 (mTORC1) or glycogen synthase kinase 3 beta (GSK-3β), respectively (Hemmings & Restuccia 2012). AKT hyperactivation in various cancers has been studied (Altomare & Testa 2005; Cheung & Testa 2012), while its role in glucose metabolism has been noted, but comparatively overlooked until analysis of AKT isoform knockout mice.

Although analogous in structure, AKT isoforms (AKT1, AKT2, and AKT3) are encoded by three different genes, which are differentially expressed in tissues and have varying functions (Hay 2011). While *Akt1* is ubiquitously expressed in mammalian tissues, it was initially deemed unnecessary for glucose homeostasis as *Akt1* knockout mice ($Akt1^{-/-}$) have impaired fetal and adulthood growth, but normal glucose tolerance and insulin signaling (Cho et al. 2001). *Akt3* is primarily expressed in the brain and was also reported unnecessary for glucose homeostasis with $Akt3^{-/-}$ mice exhibiting reduced brain size and weight, but normal glucose regulation (Tschopp et al. 2005). In contrast, *Akt2* is highly expressed in insulin responsive tissues and has been identified as a primary regulator of glucose metabolism, as *Akt2* knockout mice ($Akt2^{-/-}$) are prediabetic with insulin resistance, hyperinsulinemia, and glucose intolerance (Cho et al. 2001; Garofalo et al. 2003).

A role for AKT1 in glucose homeostasis became evident with the metabolic analysis of compound isoform knockout mice (Chen et al. 2009). Similar to $Akt2^{-/-}$ mice, $Akt1^{+/+}Akt2^{-/-}Akt3^{-/-}$ mice were mildly diabetic suggesting that the loss of *Akt3* was inconsequential. Conversely, haplodeficiency of *Akt1* in $Akt2^{-/-}$ mice resulted in a more severe diabetic phenotype, characterized by fed and fasted hyperglycemia, glucose intolerance, insulin resistance, and hyperinsulinemia. Additional crosses of $Akt1^{+/-}Akt2^{-/-}$ mice with mice haplodeficient for tumor suppressor phosphatase and tensin homolog ($PTEN^{+/-}$), an upstream regulator of AKT activation, significantly improved glucose homeostasis, and demonstrated the compensatory nature and importance of AKT1, contrary to previous reports (Cho et al. 2001). Although AKT1 hyperactivation has been frequently observed in pancreatic cancers (Schlieman et al. 2003; Missiaglia et al. 2010), there are limited studies regarding AKT1 hyperactivation and glucose homeostasis, except for attempts to improve the success rates of human islet transplantation therapy for diabetic patients (Bernal-Mizrachi et al. 2001; Tuttle et al. 2001; Kushner et al. 2005; Stiles et al. 2006;). Hyperactivation of AKT1 in pancreatic β–cells, via PTEN deletion (Kushner et al. 2005; Stiles et al. 2006) or in mice with a myristoylated *Akt1* (Bernal-Mizrachi et al. 2001; Tuttle et al. 2001) under expression of a rat insulin promoter (RIP) led to hypoglycemia, hyperinsulinemia, and improved glucose tolerance, due to increased β–cell mass, size, and proliferation.

We recently characterized aged mice with myristoylated, membrane-bound *Akt1* ($AKT1^{Myr}$) expressed using the Pdx promoter (Albury et al. 2015) and found that ~25% of mice

Author Manuscript Author Manuscript Author Manuscript Author Manuscript

developed islet cell carcinomas after one year of age. Here we report that this strain of mice exhibit non-fasted hyperglycemia as early as weaning and fasted hyperglycemia by 20 weeks of age, thus presenting a potentially unique opportunity to study the mechanistic cross-talk between diabetes and cancer. We show that the pre-diabetic phenotype can be attributed to the *Akt1*^{Myr} transgene, as it is tetracycline-regulatable, and down regulation of the *Akt1*^{Myr} transgene reduced the non-fasted and fasted hyperglycemia to wild type levels. Collectively, metabolic characterization of the AKT1^{Myr} mice revealed a novel glucagon-mediated mechanism by which AKT1 hyperactivation affects glucose homeostasis.

Materials and Methods

Animals

All mice were housed and handled according to protocols approved by the University of Central Florida (UCF) Institutional Animal Care and Use Committee at the AAALAC accredited UCF Lake Nona Animal Facility. Transgenic mice with activation of AKT1 (Pdx-tTA;TetO-MyrAkt1) were mated as previously described (Albury et al. 2015). At 3 weeks, the pups were weaned and tail snipped for DNA extraction and genotyping, as previously described (Albury et al. 2015). Mice with TetO-MyrAkt1, but lacking the knock-in Pdx-tTA, were classified as normal or wild-type litter mates. Mice with Pdx-tTA and TetO-MyrAkt1 were classified as AKT1^{Myr} mice having constitutively active AKT1 in the pancreas. Litters were placed on a standard control diet or a doxycycline diet (BioServ, Frenchtown, NJ), which shuts off *AKT1*^{Myr} transgene expression. All mice were euthanized according to American Veterinary Medical Association guidelines.

Genotyping Analysis

Primers for polymerase chain reactions (PCR) for AKT1^{Myr} mice were previously described (Albury et al. 2015). Akt2^{KO} mice were obtained from J. R. Testa (Fox Chase Cancer Center, Philadelphia, PA), and PCR primers detected the presence of wild-type or knockout *Akt2* (5′-GATGAACTTCAGGGTCAGCTT-3′; 5′-AGAGCTTCAGTGGATAGCCTA-3′; 5′-TCTCTGTCACCTCCCCATGAG-3′).

Histological Analysis

Pancreatic tissue was fixed in 10% neutral buffered formalin (Surgipath Leica, Buffalo Grove, IL) and embedded in paraffin for sectioning and processing as previously described (Albury et al. 2015). Slides were stained for hematoxylin and eosin (Surgipath) or immunohistochemistry using the Polymer Refine Detection reagents (Leica) on the Bond-Max immunostainer (Leica). Antigen retrieval was optimized using sodium citrate (pH 6) or EDTA (pH 9) buffers (Leica). The following antibodies were used: phospho-Akt Ser473 (GeneTex, Irvine, CA), also phospho-mTor Ser2448, phospho-S6 Ser235/236, glucagon, and insulin (all from Cell Signaling Technology, Danvers, MA). All slides processed on the immunostainer were run with a negative control, which was treated with antibody diluent instead of the primary antibody, to ensure antibody specificity. Images were taken using a Leica DM 2000 microscope with 5X, 10X, or 40X objectives. Islet size was measured in the whole pancreas of three mice per genotype. The mice selected had no significant lesions (NSL) at the time of necropsy, as described by a pathologist. The pancreas was sectioned

Author Manuscript Author Manuscript Author Manuscript Author Manuscript

into 5μm sections and every 25th section was H&E stained. A total of 50 islets from three sections were analyzed per mouse. Islet diameter was determined using measuring tools available on an Axio Imaging System (Zeiss, Oberkochen, Germany).

Blood Glucose Measurement

Blood glucose levels were measured using a Contour glucometer (Bayer, Mississauga, Ontario, Canada) at weaning, 5-, 7-, 9-, and 12 weeks. Weaning was at 3 weeks of age. Blood glucose levels were measured randomly, between 9 AM and 10 AM, or after an overnight fast.

Glucose Tolerance Test

Mice were fasted overnight, weighed (g), intraperitoneal (IP) injected with 2g/kg D-glucose (Fisher, Waltham, MA) and blood glucose tested with a glucometer before injection, 15-, 30-, 45-, 60-, and 120 minutes after injection. Blood glucose (mg/dL) versus time (minutes) was plotted and the area under the curve was calculated using Graph Pad Prism 5 (Graph Pad Software, La Jolla, CA). Blood was collected, via cheek bleeds, into serum collection tubes at 0 and 45 minutes after injection. The serum was separated and stored at −80°C until analysis with Mercodia Glucagon and Ultrasensitive Mouse Insulin ELISAs (Mercodia, Uppsala, Sweden). The HOMA-IR [(fasted glucose x fasted insulin)/405] was calculated using the fasted blood glucose and fasted serum insulin levels acquired during the glucose tolerance test (Grote et al. 2013).

Insulin Tolerance Testing

Mice were fasted for 2 hours, weighed (g), IP injected with 2 IU/kg porcine insulin (Sigma, Milwaukee, WI), and blood glucose tested with a glucometer before injection, 15-, 30-, 45-, and 60 minutes after injection. Blood glucose (mg/dL) versus time (minutes) was plotted and the area under the curve was calculated (GraphPad).

Insulin stimulation

Mice were fasted overnight, weighed (g), anesthetized using isoflurane, and injected with porcine insulin (10 IU/kg) (Sigma) or saline via the inferior vena cava. After two minutes mice were euthanized and the following tissues were snap frozen in liquid nitrogen: pancreas, liver, perigonadal adipose tissue, and skeletal muscle. Tissues were homogenized using 15 mg Zirconium oxide beads (1.0 mm for skeletal muscle and 0.5 mm for adipose, liver, and pancreas) with the Bullet Blender Homogenizer BBX24 (Next Advance, Averill Park, NY, USA). Proteins were extracted for ELISA analysis for AKT, AKT (pS473), Insulin Receptor (IR), and IR (pY1158) (all from Invitrogen, Camarillo, CA). Data was analyzed using a four parameter algorithm to construct the best fitting curve.

Statistical Analysis

Results are reported as mean ± SEM. Comparisons were made between two and more than two groups using unpaired or paired student's t-tests and two-way Anova followed by student's t-tests within groups, respectively. All analysis used Graph Pad Prism 5 with significance accepted at a P value of <0.05. Letters were used to illustrate significance as

Author Manuscript Author Manuscript Author Manuscript Author Manuscript

multiple groups are being compared. Groups that do not share the same letter display a statistical significance of $p<0.05$.

Results

AKT1^{Myr} transgenic mice have tetracycline-regulatable AKT/mTOR pathway activation in the pancreas

The AKT1^{Myr} construct uses the *Pdx1* promoter, which is important for pancreas development *in utero* and postnatal β-cell maintenance (Holland et al. 2002), to drive the expression of myristoylated, and therefore active *Akt1* within different pancreatic cell lineages. Expression of the *Akt1^{Myr}* transgene is inhibited in the presence of the tetracycline analogue doxycycline. Immunohistochemistry (Figure 1A), using phospho-specific antibodies, validated increased phosphorylated or active AKT1, along with its downstream substrates mTORC1 and S6, in the islets of AKT1^{Myr} mice given standard feed, as compared to wild-type mice on standard feed and doxycycline fed AKT1^{Myr} mice. To quantify this result, protein was extracted from insulin- stimulated pancreatic tissue and measured via ELISA (Figure 1B), confirming significantly elevated ($p<0.001$) AKT1 phosphorylation (Ser 473), and thus activation in AKT1^{Myr} mice versus wild type mice. Pancreatic levels of phosphorylated AKT1 (Ser 473) were eight times greater in AKT1^{Myr} mice than wild type mice, while phosphorylated AKT1 levels in doxycycline fed AKT1^{Myr} mice were equal to those of wild type mice, confirming the ability of doxycycline to turn off the transgene. Doxycycline treatment began at weaning and continued for 2 weeks, which was sufficient to decrease the activation of the AKT/mTOR pathway to wild-type levels. There was no significant difference in total AKT between groups.

Reversible, non-fasted and fasted hyperglycemia in AKT1^{Myr} transgenic mice

At weaning, mice were tail snipped for genotyping and blood glucose tested. AKT1^{Myr} mice ($n=10$), regardless of sex (Figure 2G), had significantly higher ($p<0.0001$) non-fasted blood glucose levels at weaning than wild-type littermates (Figure 2A). Non-fasted blood glucose levels were monitored biweekly for 9 weeks following weaning, and similarly, AKT1^{Myr} mice had significantly higher ($p=0.0031$) non-fasted blood glucose levels at 12 weeks of age compared to wild-type mice (Figure 2A).

To confirm that the non-fasted hyperglycemia was due to the *Akt1^{Myr}* transgene expression, doxycycline was administered to mice in order to turn off the transgene. Mating cages were arranged with half receiving standard feed and half receiving doxycycline feed for *in utero* exposure. Feeding regimens were continued at weaning and non-fasted blood glucose levels were monitored biweekly for 9 weeks. At weaning, the non-fasted blood glucose levels for AKT1^{Myr} mice on a standard diet were significantly higher ($p<0.02$) than all other treatment groups. There was no significant difference between the AKT1^{Myr} mice on doxycycline and the wild type mice on either diet, and the same pattern was observed at 12 weeks (Figure 2B). With regard to overnight fasting, 12-week AKT1^{Myr} mice exhibited no significant difference in fasted glucose levels (Figure 2C). However, aged AKT1^{Myr} exhibited fasted hyperglycemia, a more severe diabetic phenotype, by 5 months of age (Figure 2D), which

Author Manuscript Author Manuscript Author Manuscript Author Manuscript

was also attenuated by doxycycline treatment. Weight (Figure 2E) and food intake (Figure 2F) did not differ among genotypes.

Glucose intolerance in AKT1^{Myr} transgenic mice due to insulin-glucagon imbalance

Glucose tolerance testing (GTT) was performed at 12 weeks (n=5 males) to analyze the ability of AKT1^{Myr} mice to clear glucose from the blood. AKT1^{Myr} mice had a significantly higher (p=0.0049) area under the curve (Figure 3B) compared to wild-type mice. The significantly elevated blood glucose levels began at 30-minutes post injection and continued for the duration of the test, signifying glucose intolerance (Figure 3A).

Glucose intolerance in AKT1^{Myr} mice was compared and found to be similar to the well-established, prediabetic *Akt2* null mouse model (AKT2^{KO}) (Figure 3C). However, serum insulin and glucagon levels, collected via cheek bleeding, revealed significant differences between AKT1^{Myr} and AKT2^{KO} mice. AKT2^{KO} mice had significantly ($p<0.02$) elevated insulin levels, which were evident before the glucose injection (0 min) and 45 minutes after the injection (Figure 3D/Table 1). When compared to wild type mice, AKT1^{Myr} mice did not initially (0 min) have elevated insulin levels. However, insulin levels were significantly (p=0.009) higher 45 minutes after the injection. Serum glucagon levels in AKT2^{KO} mice were similar to wild type mice (Figure 3E/Table 1). However, AKT1^{Myr} mice had significantly ($p<0.05$) elevated fasted glucagon levels (0 min), which returned to wild type levels by the 45-minute time point. In addition to functional differences in pancreatic α–cells, AKT1^{Myr} mice had an altered distribution of α–cells throughout the pancreatic islets (Figure 3F), typical of several diabetic murine models (Bates et al. 2008; Cummings et al. 2008).

Insulin resistance in the liver of AKT1^{Myr} transgenic mice

One week following the GTT, an insulin tolerance test (n=5 males) was performed to analyze the sensitivity of insulin-responsive tissues in AKT1^{Myr} mice. Area under the curve was calculated (Figure 4A), blood glucose versus time, and was not significantly different when comparing AKT1^{Myr} mice and wild type mice. However, at the 15 minute time point the AKT1^{Myr} mice had significantly higher (p=0.035) blood glucose levels than the wild-type mice (Figure 4B). To further analyze insulin signaling, mice were injected with 10 IU/kg porcine insulin (n=5 males) or saline (n=5 males) via the inferior vena cava. Analysis of liver tissue revealed significantly decreased insulin receptor (IR) phosphorylation (Figure 4C) in AKT1^{Myr} mice, compared to wild type mice, despite no significant difference in insulin receptor levels. There were no differences in IR phosphorylation in adipose or muscle tissue (Figure 4D & 4E). Calculation of the homeostatic model assessment for insulin resistance (HOMA-IR) confirmed insulin resistance in AKT1^{Myr} mice, as compared to wild type mice (Figure 4F).

Decreased pancreas and islet size, with aging, in AKT1^{Myr} mice

Pancreas size was measured upon euthanization and dissection using a digital scale (n=5) in 12 week (Figure 5A) and 16 month (Figure 5B) old mice. The pancreas size in the young AKT1^{Myr} mice was not significantly different. However, the pancreas size in the aged 16 month old AKT1^{Myr} mice was significantly smaller (p=0.0049) than wild type mice. Islet

Author Manuscript Author Manuscript Author Manuscript Author Manuscript

size (n=50 islets) was also measured at 12 weeks (Figure 5C) and 16 months (Figure 5D). Islet diameter was not significantly different in 12 week old mice, but significantly decreased (p=0.008) in 16 month old mice.

Discussion

In this study we characterized the early onset, prediabetic phenotype observed in AKT1^{Myr} mice and highlighted a novel mechanism by which AKT1 hyperactivation affects glucose homeostasis. AKT1^{Myr} mice, previously described for their aged onset islet cell carcinomas (Albury et al. 2015), have bicistronic regulation of myristoylated *Akt1* through a *Pdx1-TetA* and *TetO-MyrAkt1* system. This allows the expression of myristoylated, membrane-bound and thus activated, AKT1 in the pancreas except in the presence of doxycycline, a tetracycline analogue. The *Pdx1* promoter, which is important for pancreas development *in utero* and postnatal β-cell maintenance (Holland et al. 2002), drives expression within the pancreatic progenitor cells, which eventually give rise to the endocrine cells (islets of Langerhans), exocrine cells (acini cells), and ductal cells of the pancreas (Hale et al. 2005). The hyperactivation of AKT1 throughout all cell types of the pancreas distinguishes this model from other constitutively active AKT1 mouse models, which use a rat insulin promoter (RIP) to drive expression in the β-cells (Bernal-Mizrachi et al. 2001; Tuttle et al. 2001). Additionally, the use of different tissue specific promoters highlights the important role of expression patterns and cellular localization for AKT function.

The novelty of the glucose deregulation in AKT1^{Myr} mice is further elucidated when compared to the known, prediabetic *Akt2* null mouse model (AKT2^{KO}). As previously reported, AKT2^{KO} mice have fasted and fed hyperglycemia beginning at 5- and 10 weeks in males and females, respectively (Garofalo et al. 2003). Male mice progress to a severe form of diabetes by 5 months of age and females remain prediabetic until 12 months of age (Cho H et al. 2001). Conversely, AKT1^{Myr} mice, regardless of sex, exhibited nonfasted hyperglycemia at weaning.

There was an increase in severity with time as fasted hyperglycemia was not detectable until 5 months of age. To confirm that the hyperglycemia was due to the *Akt1^{Myr}* transgene expression, doxycycline was administered to the mice to turn off the transgene. Doxycycline treatment reduced AKT1^{Myr} blood glucose to wild type levels, confirming that the fasted and non-fasted hyperglycemia in AKT1^{Myr} mice was due to AKT1 hyperactivation. Other possible contributing factors, such as weight and food intake, were ruled out further distinguishing the AKT1^{Myr} mice from the lighter AKT2^{KO} mice (Garofalo et al. 2003) and heavier obese diabetic mouse models (i.e. db/db, NZO, and TALLYHO mice) (Coleman 1982; Herberg et al. 1970; Kim et al. 2006).

Glucose tolerance testing was performed at 12 weeks to analyze the ability of AKT1^{Myr} mice to clear glucose from the blood. While both models exhibited glucose intolerance, serum insulin and glucagon levels measured during the GTT revealed that the molecular mechanisms driving the deregulations were different. As previously reported (Cho et al. 2001; Garofalo et al. 2003), AKT2^{KO} mice had hyperinsulinemia which was evident before the glucose injection and 45 minutes after the injection. Ultimately, the AKT2^{KO} mice

Author Manuscript Author Manuscript Author Manuscript Author Manuscript

model a classic, insulin-based deregulation, in which early insulin resistance leads to compensatory hyperinsulinemia, and eventually late insulin deficiency (Matthaei et al. 2000). When compared to wild type mice, AKT1^{Myr} mice did not have elevated fasted insulin levels. However, insulin levels were significantly higher 45 minutes after the injection. This increase in insulin secretion may be β-cell compensation and occurred in response to the hyperglycemia also observed at this time point. This suggests that the elevated blood glucose levels were not due to a lack of insulin production or secretion, but reduced insulin sensitivity (Weir & Bonner-Weir 2004).

While insulin deregulations are well studied, glucagon deregulations have been acknowledged but relatively ignored. Glucagon, which is secreted by pancreatic α–cells when blood glucose levels are low, is known as the antagonist to insulin. When glucagon binds to its receptor it activates cellular adenosine-3′-5′-cyclic monophosphate (cAMP) and protein kinase A (PKA) signaling to induce hepatic gluconeogenesis and glycogenolysis restoring glucose homeostasis during fasting (Moon & Won 2015). Increased PKA activity impairs glucose stimulated insulin secretion (GSIS), which is needed to prevent the immediate secretion and glucose disposing action of insulin (Song et al. 2014). Serum glucagon levels in AKT2^{KO} mice were similar to wild type mice. However, AKT1^{Myr} mice had significantly elevated fasted glucagon levels, which returned to wild type levels by the 45-minute time point, most likely due to the surge in insulin secretion.

Fasted hyperglucagonemia, as seen in AKT1^{Myr} mice, has been observed in diabetic patients (Baron et al. 1987; Reaven et al. 1987; Unger et al. 1970), and linked to the manifestation of fasted hyperglycemia and glucose intolerance. The mechanisms behind hyperglucagonemia are still relatively unclear, but it has been shown to result from the inadequate response of α–cells to elevated blood glucose levels (Rizza 2010). This α–cell dysfunction leads to hepatic insulin resistance (Basu et al. 2004), causing non-fasted hyperglycemia by preventing the suppression of endogenous glucose production during a meal, and fasted hyperglycemia via chronically elevated endogenous glucose production (Basu et al. 2000; Firth et al. 1986). The hyperglucagonemia induced hepatic insulin resistance also significantly decreases hepatic glucose uptake and disposal due to impaired glucokinase activity (Caro et al. 1995; Wajngot et al. 1991). This impaired hepatic glucose metabolism has been identified in mild and severe diabetes patients making it an early contributing event in the pathogenesis of diabetes, and not simply an effect (Basu et al. 2004; Bock et al. 2007).

One week following the GTT, an insulin tolerance test was performed to analyze the sensitivity of insulin-responsive tissues in AKT1^{Myr} mice. AKT1^{Myr} mice and wild type mice were not significantly different when comparing area under the curve, suggesting an absence of insulin resistance. However, at the 15 minute time point the AKT1^{Myr} mice had significantly higher blood glucose levels than the wild-type mice, suggesting there may be altered insulin signaling causing this delay in insulin response. Further analysis of liver tissue revealed significantly decreased insulin receptor (IR) phosphorylation in AKT1^{Myr} mice, compared to wild type mice, despite no significant difference in insulin receptor levels. This decrease in IR activation explains the delay in insulin response seen early in the ITT and the inability of AKT1^{Myr} mice to aptly clear glucose from the blood. Further calculation of the HOMA-IR confirmed insulin resistance in AKT1^{Myr} mice, as compared to

Author Manuscript Author Manuscript Author Manuscript Author Manuscript

wild type mice. However, at 12 weeks, this resistance is not as severe as the resistance seen in $AKT2^{KO}$ mice.

Additional longevity studies must be performed to determine whether the insulin resistance worsens with age, but analysis of pancreas and islet size suggests a gradual loss of β-cell mass. This loss of β-cell mass, evident by a decrease in total pancreas size and islet diameter, is typically indicative of long term insulin resistance and β-cell failure due to chronic hyperinsulinemia and hyperglycemia (Prentki & Nolan 2006). There also appears to be an age induced increase in islet diameter of wild type mice. This is most likely due to naturally occurring beta-cell compensation or the presence of islet adenomas which also develop naturally in about 33% of our aged wild type mice.

In this study we characterized the pre-tumor, prediabetic phenotype of $AKT1^{Myr}$ mice, which exhibit non-fasted hyperglycemia as early as weaning and fasted hyperglycemia by 5 months of age, regardless of sex. Based upon previous findings, this hyperglycemia is likely due to α-cell dysfunction, specifically hyperglucagonemia. Although the mechanisms behind hyperglucagonemia are still relatively unclear, we are proposing that $AKT1^{Myr}$ mice, with fasted hyperglucagonemia, have impaired GSIS, resulting in glucose intolerance despite increased compensatory insulin secretion. Hepatic insulin resistance, an additional factor, may exacerbate the problem, preventing normoglycemia via increased hepatic glucose production and decreased hepatic glucose storage. As the fasted and non-fasted hyperglycemias are reversible when the $Akt1^{Myr}$ transgene is suppressed we have attributed this diabetic phenotype to the constitutive activation of AKT1 in the pancreas of this mouse model. Collectively, this pre-diabetic model highlights a novel glucagon-mediated mechanism by which AKT1 hyperactivation affects glucose homeostasis, and provides a means to better delineate molecular mechanisms contributing to diabetes mellitus, and perhaps future association between diabetes and a subset of pancreatic cancers.

Acknowledgments

Funding

This work was supported by the National Cancer Institute (NCI) grant R21 (CA129302 to D.A.A.); the University of Central Florida (UCF) Gerontology Applied Research Fellowship from the Learning Institute for Elders at UCF (MEDI00041); the Florida Ladies Auxiliary to the Veterans of Foreign Wars (MEDI000177); the UCF Burnett School of Biomedical Sciences Startup Funds (20070716) and the National Institute on Aging (AG032290 to M.M.M.). TMA was supported in part by a McKnight Graduate Fellowship provided by the Florida Education Fund.

R21 CA129302 supported the initial studies of glucose deregulation. Completion of the work was supported by donations from the Learning Institute for Elders at UCF and the Florida Ladies Auxiliary to the Veterans of Foreign Wars. BSBS shared core equipment resources for histology and UCF animal care facilities were used for this study.

References

1. Albury TM, Pandey V, Gitto SB, Dominguez L, Spinel LP, Talarchek J, Klein-Szanto AJ, Testa JR, Altomare DA. Constitutive activation of Akt1 cooperates with KRasG12D to accelerate in vivo pancreatic tumor onset and progression. Neoplasia. 2015; 17:175–183. [PubMed: 25748236]
2. Altomare DA, Testa JR. Perturbations of the AKT signaling pathway in human cancer. Oncogene. 2005; 24:7455–7464. [PubMed: 16288292]

Author Manuscript Author Manuscript Author Manuscript Author Manuscript

3. Baron AD, Schaeffer L, Shragg P, Kolterman OG. Role of hyperglucagonemia in maintenance of increased rates of hepatic glucose output in type II diabetics. Diabetes. 1987; 36:274–283. [PubMed: 2879757]
4. Basu A, Basu R, Shah P, Vella A, Johnson CM, Nair KS, Jensen MD, Schwenk WF, Rizza RA. Effects of type 2 diabetes on the ability of insulin and glucose to regulate splanchnic and muscle glucose metabolism: evidence for a defect in hepatic glucokinase activity. Diabetes. 2000; 49:272–283. [PubMed: 10868944]
5. Basu R, Basu A, Johnson CM, Schwenk WF, Rizza RA. Insulin dose-response curves for stimulation of splanchnic glucose uptake and suppression of endogenous glucose production differ in nondiabetic humans and are abnormal in people with type 2 diabetes. Diabetes. 2004; 53:2042–2050. [PubMed: 15277384]
6. Basu R, Schwenk WF, Rizza RA. Both fasting glucose production and disappearance are abnormal in people with “mild” and “severe” type 2 diabetes. Am J Physiol Endocrinol Metab. 2004; 287:E55–E62. [PubMed: 14982753]
7. Bates H, Sirek A, Kiraly M, Yue J, Riddell M, Matthews S, Vranic M. Adaptation to intermittent stress promotes maintenance of beta-cell compensation: comparison with food restriction. Am J Physiol Endocrinol Metab. 2008; 295:E947–58. [PubMed: 18713962]
8. Bernal-Mizrachi E, Wen W, Stahlhut S, Welling CM, Permutt MA. Islet beta cell expression of constitutively active Akt1/PKB alpha induces striking hypertrophy, hyperplasia, and hyperinsulinemia. J Clin Invest. 2001; 108:1631–1638. [PubMed: 11733558]
9. Bock G, Chittilapilly E, Basu R, Toffolo G, Cobelli C, Chandramouli V, Landau BR, Rizza RA. Contribution of hepatic and extrahepatic insulin resistance to the pathogenesis of impaired fasting glucose: role of increased rates of gluconeogenesis. Diabetes. 2007; 56:1703–1711. [PubMed: 17384334]
10. Caro JF, Triester S, Patel VK, Tapscott EB, Frazier NL, Dohm GL. Liver glucokinase: decreased activity in patients with type II diabetes. Horm Metab Res. 1995; 27:19–22. [PubMed: 7729787]
11. Chen WS, Peng XD, Wang Y, Xu PZ, Chen ML, Luo Y, Jeon SM, Coleman K, Haschek WM, Bass J, et al. Leptin deficiency and beta-cell dysfunction underlie type 2 diabetes in compound Akt knockout mice. Mol Cell Biol. 2009; 29:3151–3162. [PubMed: 19289493]
12. Cheung M, Testa JR. Diverse mechanisms of AKT pathway activation in human malignancy. Curr Cancer Drug Targets. 2013; 13:234–244. [PubMed: 23297823]
13. Cho H, Mu J, Kim JK, Thorvaldsen JL, Chu Q, Crenshaw EB, Kaestner KH, Bartolomei MS, Shulman GI, Birnbaum MJ. Insulin resistance and a diabetes mellitus-like syndrome in mice lacking the protein kinase Akt2 (PKB beta). Science. 2001; 292:1728–1731. [PubMed: 11387480]
14. Cho H, Thorvaldsen JL, Chu Q, Feng F, Birnbaum MJ. Akt1/PKBalpha is required for normal growth but dispensable for maintenance of glucose homeostasis in mice. J Biol Chem. 2001; 276:38349–38352. [PubMed: 11533044]
15. Coleman DL. Diabetes-obesity syndromes in mice. Diabetes. 1982; 31:1–6. [PubMed: 7160533]
16. Cummings B, Digitale E, Stanhope K, Graham J, Baskin D, Reed B, Sweet I, Griffen S, Havel PJ. Development and characterization of a novel rat model of type 2 diabetes mellitus: the UC Davis type 2 diabetes mellitus UCD-T2DM rat. Am J Physiol Regul Integr Comp Physiol. 2008; 295:1782–1793.
17. Firth RG, Bell PM, Marsh HM, Hansen I, Rizza RA. Postprandial hyperglycemia in patients with noninsulin-dependent diabetes mellitus. Role of hepatic and extrahepatic tissues. J Clin Invest. 1986; 77:1525–1532. [PubMed: 3517067]
18. Garofalo RS, Orena SJ, Rafidi K, Torchia AJ, Stock JL, Hildebrandt AL, Coskran T, Black SC, Brees DJ, Wicks JR, et al. Severe diabetes, age-dependent loss of adipose tissue, and mild growth deficiency in mice lacking Akt2/PKB beta. J Clin Invest. 2003; 112:197–208. [PubMed: 12843127]
19. Grote CW, Groover AL, Ryals JM, Geiger PC, Feldman EL, Wright DE. Peripheral nervous system insulin resistance in ob/ob mice. Acta Neuropathol Commun. 2013; 1:1–11.
20. Hale MA, Kagami H, Shi L, Holland AM, Elsässer HP, Hammer RE, MacDonald RJ. The homeodomain protein PDX1 is required at mid-pancreatic development for the formation of the exocrine pancreas. Dev Biol. 2005; 286:225–237. [PubMed: 16126192]

Author Manuscript Author Manuscript Author Manuscript Author Manuscript

21. Hay N. Akt isoforms and glucose homeostasis - the leptin connection. Trends Endocrinol Metab. 2011; 22:66–73. [PubMed: 20947368]
22. Hemmings BA, Restuccia DF. PI3K-PKB/Akt pathway. Cold Spring Harb Perspect Biol. 2012; 4:1–3.
23. Herberg L, Major E, Hennigs U, Grüneklee D, Freytag G, Gries FA. Differences in the development of the obese-hyperglycemic syndrome in obob and NZO mice. Diabetologia. 1970; 6:292–298. [PubMed: 4914666]
24. Holland AM, Hale MA, Kagami H, Hammer RE, MacDonald RJ. Experimental control of pancreatic development and maintenance. Proc Natl Acad Sci. 2002; 99:12236–12241. [PubMed: 12221286]
25. Kim JH, Stewart TP, Soltani-Bejnood M, Wang L, Fortuna JM, Mostafa OA, Moustaid-Moussa N, Shoieb AM, McEntee MF, Wang Y, et al. Phenotypic characterization of polygenic type 2 diabetes in TALLYHO/JngJ mice. J Endocrinol. 2006; 191:437–446. [PubMed: 17088413]
26. Kushner JA, Simpson L, Wartschow LM, Guo S, Rankin MM, Parsons R, White MF. Phosphatase and tensin homolog regulation of islet growth and glucose homeostasis. J Biol Chem. 2005; 280:39388–39393. [PubMed: 16170201]
27. Matthaei S, Stumvoll M, Kellerer M, Häring HU. Pathophysiology and pharmacological treatment of insulin resistance. Endocr Rev. 2000; 21:585–618. [PubMed: 11133066]
28. Missiaglia E, Dalai I, Barbi S, Beghelli S, Falconi M, della Peruta M, Piemonti L, Capurso G, Di Florio A, delle Fave G, et al. Pancreatic endocrine tumors: expression profiling evidences a role for AKT-mTOR pathway. J Clin Oncol. 2010; 28:245–255. [PubMed: 19917848]
29. Moon JS, Won KC. Pancreatic α-Cell Dysfunction in Type 2 Diabetes: Old Kids on the Block. Diabetes Metab J. 2015; 39:1–9. [PubMed: 25729706]
30. Prentki M, Nolan CJ. Islet beta cell failure in type 2 diabetes. J Clin Invest. 2006; 116:1802–1812. [PubMed: 16823478]
31. Reaven GM, Chen YD, Golay A, Swislocki AL, Jaspan JB. Documentation of hyperglucagonemia throughout the day in nonobese and obese patients with noninsulin-dependent diabetes mellitus. J Clin Endocrinol Metab. 1987; 64:106–110. [PubMed: 3536980]
32. Rizza RA. Pathogenesis of fasting and postprandial hyperglycemia in type 2 diabetes: implications for therapy. Diabetes. 2010; 59:2697–2707. [PubMed: 20705776]
33. Schlieman MG, Fahy BN, Ramsamooj R, Beckett L, Bold RJ. Incidence, mechanism and prognostic value of activated AKT in pancreas cancer. Br J Cancer. 2003; 89:2110–2115. [PubMed: 14647146]
34. Song WJ, Mondal P, Wolfe A, Alonso LC, Stamateris R, Ong BW, Lim OC, Yang KS, Radovick S, Novaira HJ, et al. Glucagon regulates hepatic kisspeptin to impair insulin secretion. Cell Metab. 2014; 19:667–681. [PubMed: 24703698]
35. Stiles BL, Kuralwalla-Martinez C, Guo W, Gregorian C, Wang Y, Tian J, Magnuson MA, Wu H. Selective deletion of Pten in pancreatic beta cells leads to increased islet mass and resistance to STZ-induced diabetes. Mol Cell Biol. 2006; 26:2772–2781. [PubMed: 16537919]
36. Tschopp O, Yang ZZ, Brodbeck D, Dummler BA, Hemmings-Mieszczak M, Watanabe T, Michaelis T, Frahm J, Hemmings BA. Essential role of protein kinase B gamma (PKB gamma/Akt3) in postnatal brain development but not in glucose homeostasis. Development. 2005; 132:2943–2954. [PubMed: 15930105]
37. Tuttle RL, Gill NS, Pugh W, Lee JP, Koeberlein B, Furth EE, Polonsky KS, Naji A, Birnbaum MJ. Regulation of pancreatic beta-cell growth and survival by the serine/threonine protein kinase Akt1/PKBalpha. Nat Med. 2001; 7:5–14. [PubMed: 11135587]
38. Unger RH, Aguilar-Parada E, Müller WA, Eisentraut AM. Studies of pancreatic alpha cell function in normal and diabetic subjects. J Clin Invest. 1970; 49:837–848. [PubMed: 4986215]
39. Wajngot A, Chandramouli V, Schumann WC, Efendic S, Landau BR. Quantitation of glycogen/glucose-1-P cycling in liver. Metabolism. 1991; 40:877–881. [PubMed: 1861637]
40. Weir GC, Bonner-Weir S. Five stages of evolving beta-cell dysfunction during progression to diabetes. Diabetes. 2004; 53:16–21.

Author Manuscript Author Manuscript Author Manuscript Author Manuscript

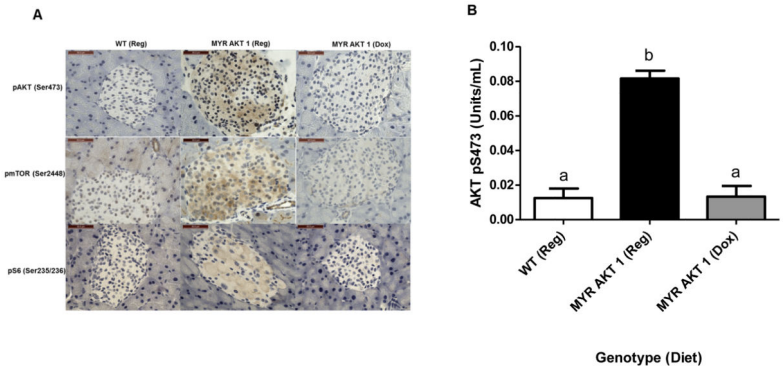

Figure 1. AKT1^{Myr} mice have doxycycline-regulatable AKT/mTOR pathway activation in the pancreas

Hyperactivation and decreased activation of the AKT/mTOR pathway in AKT1^{Myr} mice on regular chow diet and AKT1^{Myr} mice on doxycycline diet, respectively, confirmed with: (A) immunostaining of representative pancreatic tissue using phospho-AKT (Ser 473), phospho-mTOR (Ser 2448), and phospho-S6 (Ser 235/236) antibodies (40X objective; Scale bar-50μm); and (B) analysis of protein from pancreatic tissue using a phospho-AKT1 (Ser 473) ELISA. Two-way ANOVA followed by student's t-tests within groups were used to analyze the data. Data represented as mean ± SEM (n=5). All phospho-AKT1 measurements were normalized to their total AKT measurements. Abbreviations: WT – wild type mice; Reg-regular chow diet; Dox - doxycycline diet. Letters were used to illustrate significance as multiple groups are being compared (see materials and methods for explanation).

Author Manuscript Author Manuscript Author Manuscript Author Manuscript

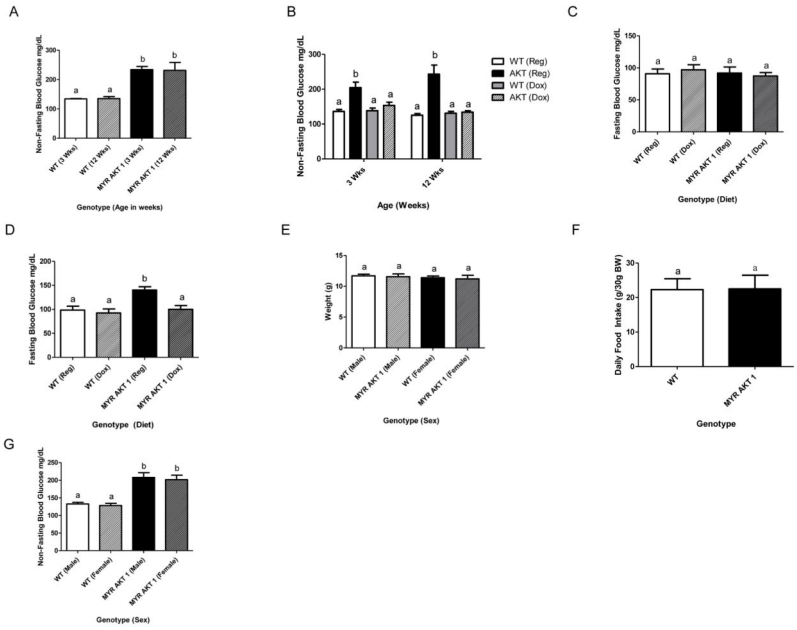

Figure 2. AKT1^{Myr} mice have a reversible, fasted and non-fasted hyperglycemia

Blood glucose levels were measured with a glucometer (A) at weaning ($p<0.0001$) and at 12 weeks ($p=0.0031$). Weaning occurred at 3 weeks of age. To determine if the hyperglycemia exhibited at weaning was reversible, breeder mice were placed on a doxycycline diet to expose the pups *in utero*. Blood glucose levels were then measured (B) at weaning ($p<0.02$) and at 12 weeks ($p\leq0.003$). Mice were fasted overnight (16 hours) to determine fasted blood glucose levels (C) at 12 weeks and (D) at 20 weeks ($p<0.005$). (E) Weight was measured at weaning. At 12 weeks, mice were housed individually and (F) food intake was measured daily for four days by weighing the food in the cage. Blood glucose levels, measured at weaning, were used to identify (G) sex differences. Two-way ANOVA followed by student's t-tests within groups were used to analyze the data for figures 2A–E and 2G. Unpaired student's t-test was used for figure 2F. N=10 for figures A–G except D (n=5). Abbreviations: Wks - week. Letters were used to illustrate significance as multiple groups are being compared (see materials and methods for explanation).

Author Manuscript Author Manuscript Author Manuscript Author Manuscript

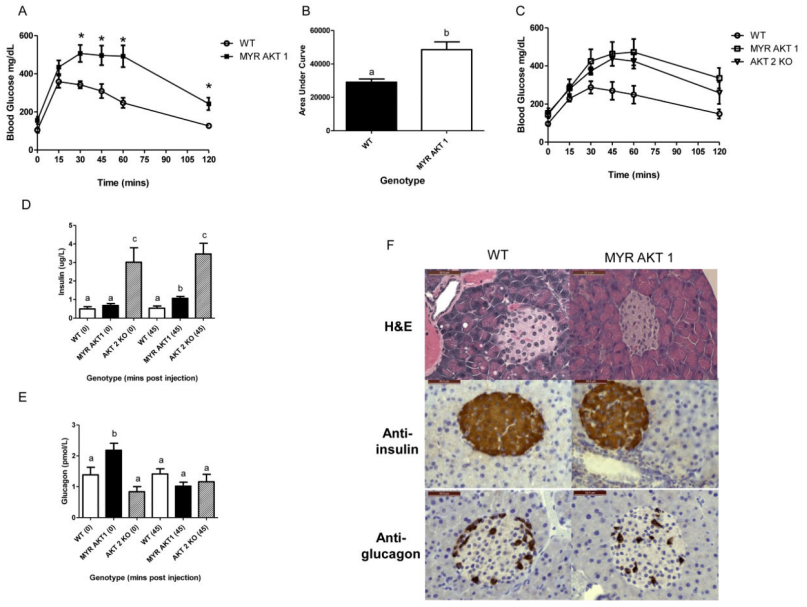

Figure 3. Glucose intolerance in AKT1^{Myr} mice due to insulin-glucagon imbalance

Glucose tolerance testing (n=5) was performed at 12 weeks comparing: (A) wild type (WT) and AKT1^{Myr} (MYR AKT1) mice and (C) WT, MYR AKT1, and Akt2$^{-/-}$ (AKT2 KO) mice (* indicates $p<0.05$). (B) Area under the curve. Data represented as mean ± SEM ($p=0.0049$). Blood was collected, via cheek bleeds, at the 0- and 45-minute timepoints to analyze serum (D) insulin and (E) glucagon levels using ELISAs. Insulin and glucagon values are also provided in Table 1. (F) Immunostaining of pancreatic tissue using insulin and glucagon antibodies (Objective 40X; Scale bar-50μm). Unpaired student's t-tests were used to analyze differences in area under the curve and the glucose tolerance test time points. Two-way ANOVA followed by student's t-tests within groups were used to analyze the data for figures 3D–E. Letters were used to illustrate significance as multiple groups are being compared (see materials and methods for explanation).

Author Manuscript Author Manuscript Author Manuscript Author Manuscript

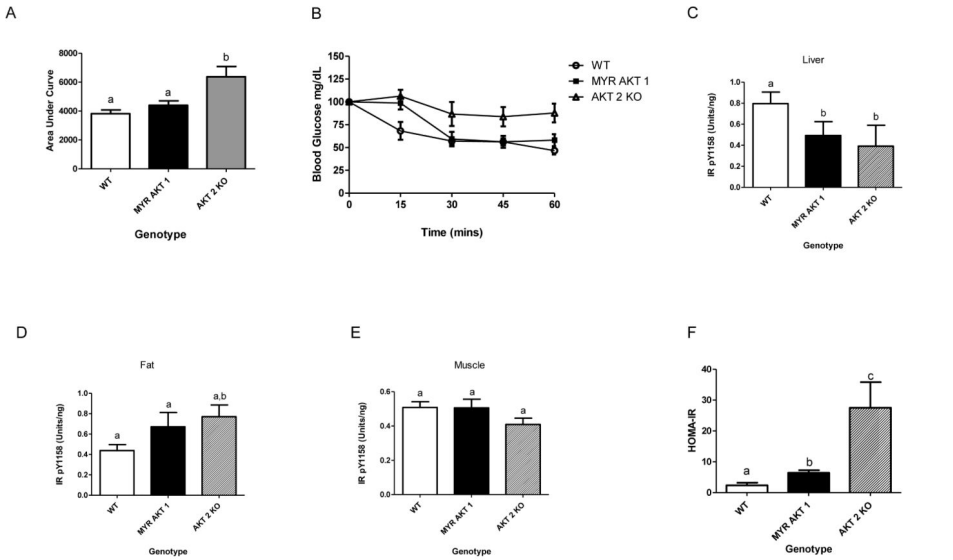

Figure 4. Insulin resistance in the liver of AKT1^{Myr} mice

One week following the GTT, (B) an insulin tolerance test was performed (n=5). (A) Area under the curve. Data represented as mean ± SEM ($p<0.04$). To analyze insulin signaling, mice were insulin stimulated. Two minutes after injection the mice were euthanized and the pancreas, (C) liver, (D) adipose tissue, and (E) skeletal muscle were collected, protein extracted, and analyzed with insulin receptor (IR) Total and IR (pY1158) ELISAs. All phospho-IR measurements were normalized to their total IR measurements. (F) Homeostatic model assessment for insulin resistance (HOMA-IR) was calculated using the following measurements from the GTT: (fasted glucose x fasted insulin)/405. Data represented as mean ± SEM. Unpaired student's t-tests were used to analyze differences in the insulin tolerance tests time points. One-way ANOVA followed by student's t-tests within groups were used to analyze the data for figures 4A and 4C–F. Letters were used to illustrate significance as multiple groups are being compared (see materials and methods for explanation).

Author Manuscript Author Manuscript Author Manuscript Author Manuscript

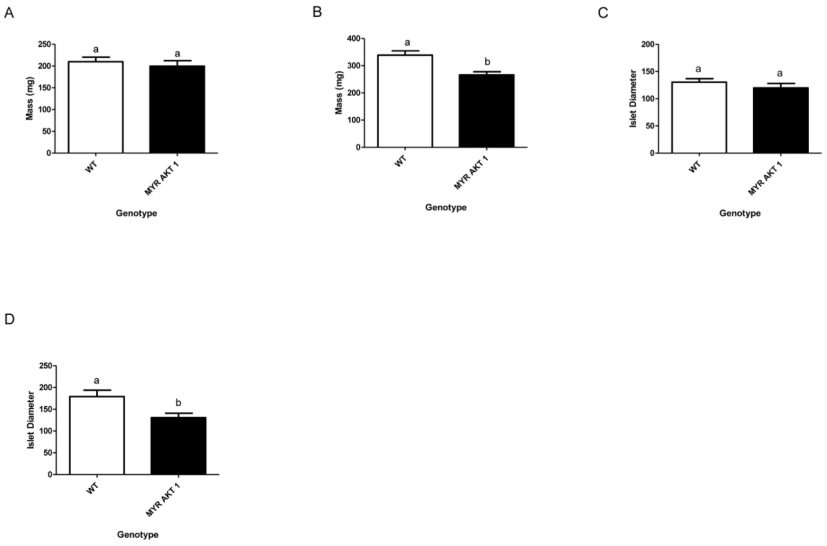

Figure 5. Decreased pancreas and islet size, with aging, in AKT1^{Myr} mice

Pancreas size was measured upon euthanization and dissection using a digital scale (n=5) in (A) 12 week and (B) 16 month (p=0.0049) old mice. Islet size (n=50 islets) was also measured at (C) 12 weeks and (D) 16 months (p=0.008). Islet diameter was determined analyzing H&E stained sections through Axio Imaging Software. Unpaired student's t-tests were used to analyze figures 5A–D. Data represented as mean ± SEM. Letters were used to illustrate significance as multiple groups are being compared (see materials and methods for explanation).

Author Manuscript

Author Manuscript

Author Manuscript

Author Manuscript

Table 1

The average insulin and glucagon serum levels in wild type, MYR AKT1, and AKT2 KO mice during the glucose tolerance test.

	Average Insulin Levels (μg/L)		
Minutes Post Glucose Injection	**Wild Type**	**MYR AKT1**	**AKT2 KO**
0 minutes	0.50	0.68	*3.0 (p<0.02)
45 minutes	0.54	* 1.1 (p=0.009)	*3.5 (p<0.02)
	Average Glucagon Levels (pmol/L)		
0 minutes	1.38	* 2.18 (p<0.05)	0.84
45 minutes	1.42	1.02	1.16

* Indicates a significant difference. The data in this table corresponds to panels D and E in Figure 3.